Sun Zhentao (Orcid ID: 0000-0001-7606-0278)
Ouyang Zhangxian (Orcid ID: 0000-0002-0173-0377)
Hussain Najid (Orcid ID: 0000-0003-0062-4414)
Cai Wei - Jun (Orcid ID: 0000-0003-3606-8325)

Simultaneous Onboard Analysis of Seawater Dissolved Inorganic Carbon (DIC) Concentration and Stable Isotope Ratio (δ^{13}C-DIC)

Running head: Onboard analysis of seawater DIC and δ^{13}C-DIC

*Zhentao Sun[1], Xinyu Li[1,2], Zhangxian Ouyang[1], Charles Featherstone[3], Eliot A. Atekwana[4], Najid Hussain[1], and Wei-Jun Cai[1,]**

[1] School of Marine Science and Policy, University of Delaware, Newark, Delaware 19716, USA

[2] Cooperative Institute for Climate Ocean and Ecosystem Studies (CICOES), University of Washington, Seattle, Washington 98105, USA

[3] Atlantic Oceanographic and Meteorological Laboratory, National Oceanic and Atmospheric Administration, 4301 Rickenbacker Causeway, Miami, Florida 33149, USA

[4] Department Earth and Planetary Sciences, University of California Davis, Davis, California 95616, USA

* Corresponding author, e-mail address: wcai@udel.edu

This is the author manuscript accepted for publication and has undergone full peer review but has not been through the copyediting, typesetting, pagination and proofreading process, which may lead to differences between this version and the Version of Record. Please cite this article as doi: 10.1002/lom3.10642

Abstract

Dissolved inorganic carbon (DIC) and stable carbon isotope (δ^{13}C-DIC) are valuable parameters for studying the aquatic carbon cycle and quantifying ocean anthropogenic carbon accumulation rates. However, the potential of this coupled pair is underexploited as only 15 % or less of cruise samples have been analyzed for δ^{13}C-DIC because the traditional isotope analysis is labor-intensive and restricted to onshore laboratories. Here, we improve the analytical precision and reported the protocol of an automated, efficient, and high-precision method for ship-based DIC and δ^{13}C-DIC analysis based on Cavity Ring-Down Spectroscopy (CRDS). We also introduced a set of stable in-house standards to ensure accurate and consistent DIC and δ^{13}C-DIC measurements, especially on prolonged cruises. With this method, we analyzed over 1600 discrete seawater samples over a 40-day cruise along the North American eastern ocean margin in summer 2022, representing the first effort to collect a large dataset of δ^{13}C-DIC onboard of any oceanographic expedition. We evaluated the method's uncertainty, which was 1.2 μmol kg^{-1} for the DIC concentration and 0.03 ‰ for the δ^{13}C-DIC value (1σ). An interlaboratory comparison of onboard DIC concentration analysis revealed an average offset of 2.0 ± 3.8 μmol kg^{-1} between CRDS and the coulometry-based results. The cross-validation of δ^{13}C-DIC in the deep-ocean data exhibited a mean difference of only –0.03 ± 0.07 ‰, emphasizing the consistency with historical data. Potential applications in aquatic biogeochemistry are discussed.

Keywords

dissolved inorganic carbon; stable carbon isotope; cavity ring-down spectroscopy; onboard measurement; discrete sample; US Atlantic Ocean margin

Introduction

Since the Industrial Revolution, oceans have absorbed ~ 25 % of anthropogenic CO_2 (Friedlingstein et al. 2023; Le Quéré et al. 2009), increasing seawater dissolved inorganic carbon (DIC) concentration and lowering pH, altering biogeochemistry and endangering carbonate-bearing organisms. High-resolution DIC concentration measurements are key for marine studies (Carter et al. 2019), yet tracking oceanic anthropogenic carbon changes solely through DIC increase is limited due to minor changes against high background levels and large spatiotemporal variability (Doney et al. 2009). The $^{13}C/^{12}C$ ratio of oceanic DIC (δ^{13}C-DIC), influenced by the ^{13}C depleted CO_2 from fossil fuel burning (the Suess effect), can serve as an effective marker for estimating oceanic anthropogenic CO_2 changes (Keeling 1979; Lynch-Stieglitz et al. 1995). In particular, Quay and co-workers proposed that $\delta^{13}C$ could be a more sensitive tracer than DIC for quantifying anthropogenic CO_2 accumulation rates in the ocean due to a stronger anthropogenic perturbation than natural spatiotemporal variability (Körtzinger et al. 2003; Quay et al. 2017; Quay et al. 2007; Quay et al. 2003; Sonnerup and Quay 2012). Moreover, δ^{13}C-DIC can offer an estimate of net community production (Quay et al. 2009; Yang et al. 2019) and aid in distinguishing DIC sources and sinks (Samanta et al. 2015), elucidating DIC dynamics across estuaries and coastal waters (Kwon et al. 2021; Yang et al. 2018).

The lack of δ^{13}C-DIC data limits understanding of marine carbonate system changes, with only 15 % of the ocean basin and fewer coastal samples analyzed for δ^{13}C-DIC compared to DIC (Bauer et al. 2001; Becker et al. 2016). This scarcity results from the high costs and extensive labor associated with traditional Isotope Ratio Mass Spectrometry (IRMS) analysis, along with the demanding requirements for space and careful handling in the preservation and transportation of samples from shipboard to shore-based laboratories. Recent developments in laser-based

optical spectroscopy, like Cavity Ring-Down Spectroscopy (CRDS), have achieved a short-term laboratory precision to 1.5 μmol kg^{-1} for DIC concentration and 0.09 ‰ for δ^{13}C-DIC (Call et al. 2017; Su et al. 2019), approaching the guidelines of essential ocean variables set by the Global Ocean Observing System (GOOS), precisely, ± 2 μmol kg^{-1} for DIC concentration and ± 0.05 ‰ for δ^{13}C-DIC. Until now, most δ^{13}C-DIC analyses remain restricted to land-based laboratories, with storage and transportation introducing potential accuracy-reducing artifacts. Delays in processing at high-quality facilities further exacerbate this issue (Humphreys et al. 2015) with accuracy potentially dropping by about 0.1 ‰ after six months and nearly 0.2 ‰ after 18 months of storage (Olack et al. 2018).

Challenges in expanding the application of CRDS-based instruments for onboard measurements come from the manual and time-intensive procedures to handle the large volume of samples. Becker et al. (2012) first used a continuous wave CRDS analyzer linking to an air-sea equilibrator onboard for underway δ^{13}C measurements of the oceanic CO_2. However, converting the δ^{13}C-CO_2 values to δ^{13}C-DIC values required additional calculations based on the isotope fractionation, potentially introducing errors from fractionation factor determination across various conditions (Zhang et al. 1995), limiting the uncertainty to ± 0.35 ‰ (Becker et al. 2012). Su et al. (2019) developed a novel analyzer by coupling a CO_2 acidification and extraction device with a CRDS detector to simultaneously measure DIC concentration and δ^{13}C-DIC values. Building on this work, Deng et al. (2022) enhanced the method by incorporating a multi-port valve, enabling automatic sample loading and measurement. Nevertheless, the applicability of this approach for extended maritime expeditions remains unassessed and further improvement on the precision is desirable. The absence of stable in-house standards or commercial reference solutions for seawater δ^{13}C-DIC ranges is a key restriction for the

precision and accuracy of shipboard measurements (Cheng et al. 2019). Addressing systematic drift in δ^{13}C-DIC over extended, uninterrupted long-term measurements remains essential.

This study introduces a protocol based on the CRDS-based analyzer for onboard DIC and δ^{13}C-DIC analysis, detailing its uncertainty and operational efficiency during a 40-day expedition along the North American eastern ocean margin. Successfully analyzing 1666 samples at 30 samples per day per analyzer, this work represents the first collection of an extensive δ^{13}C-DIC dataset on a long cruise. Our results also affirm the consistency and reliability of in-house sodium bicarbonate ($NaHCO_3$) solutions, and the certified reference material (CRM) for oceanic CO_2 measurements from Scripps Institute of Oceanography (Dickson et al. 2007) as reference standards for δ^{13}C-DIC.

Materials and procedure

Preparation of in-house standards

We employed three seawater-like $NaHCO_3$ solutions with δ^{13}C-DIC values around –1 ‰ (SB-1), –4 ‰ (SB-2), and 1 ‰ (SB-3) as in-house reference materials. These were used to accurately measure DIC concentrations and δ^{13}C-DIC values, aligning with the oceanic δ^{13}C-DIC range of –4 ‰ to 3 ‰, especially within the narrower range of most Atlantic waters (Cheng et al. 2019). All δ^{13}C values reported in this study are expressed relative to the reference standard Vienna PeeDee Belemnite (V-PDB).

To prepare SB-1 and SB-2 standards, we dissolved baking soda ($NaHCO_3$) from Best Yet® (USA) and ARM & HAMMER™ (USA) with δ^{13}C values of –0.99 ‰ and –4.19 ‰, respectively, in ultrapure water (resistivity 18.2 MΩ cm) purged with CO_2-free air. Addressing two challenges, the unavailability of commercial $NaHCO_3$ with $\delta^{13}C > 0$ ‰, and the poor solubility of isotopically heavy calcite ($CaCO_3$) in seawater-like solutions, we developed an in-

house standard (SB-3) by mixing –0.99 ‰ valued baking soda and ^{13}C labeled $NaHCO_3$ (99 % atom % ^{13}C, Cambridge Isotope Laboratories, USA), following the procedure detailed in Appendix S1. Briefly, 0.012 g of ^{13}C labeled $NaHCO_3$ was dissolved in 10 mL of CO_2-free water for the stock solution. We mixed 100 μL of this stock with 5.000 g of the baking soda in CO_2-free water for an expected $\delta^{13}C$-DIC value of 1.12 ‰. We adjusted the DIC concentration of all in-house standards to ~ 2000 μmol L^{-1}. The in-house standards were preserved with saturated $HgCl_2$ (0.025 % vol./vol.) and stored in 4 L aluminum-coated, gas-tight bags (Calibrated Instruments Inc., USA), ceasing use when the volume reduced to one-sixth of 4 L to minimize the impacts of gas exchange and possible other changes.

We aged all in-house standards for one month before usage. This process allowed us to: (a) verify that the $\delta^{13}C$-DIC values of our standards remained constant during storage, (b) ensure complete isotopic equilibration within the solution, and (c) detect any potential contamination. The DIC concentrations of in-house standards were regularly calibrated against CRMs from Batch #197 (2115.23 ± 0.53 μmol kg^{-1}) and #199 (2021.66 ± 0.52 μmol kg^{-1}). Detailed information about these batches is available on the Ocean Carbon and Acidification Data System (OCADS) website (https://www.ncei.noaa.gov/access/ocean-carbon-acidification-data-system/oceans/Dickson_CRM/batches.html). Additionally, we subsampled in-house standards into 12 mL Exetainer® vials (Labco Limited, UK) weekly at sea to check their stability during usage. Once back on land, these vials were sent to University of California Davis Stable Isotope Facility for $\delta^{13}C$-DIC analysis using the headspace equilibration technique (Atekwana and Krishnamurthy 1998), employing a GasBench II system linked to a Delta Plus XL IRMS (Thermo Scientific, Bremen, Germany). These IRMS-derived $\delta^{13}C$-DIC values then were used to calibrate our CRDS $\delta^{13}C$-DIC measurements.

Collection of seawater samples

During the ship-based repeated hydrographic observations, discrete seawater samples for DIC and δ^{13}C-DIC were collected according to best practices (Dickson et al. 2007) from a profiling Conductivity, Temperature, and Depth (CTD) instrument paired with Niskin bottles. One or two duplicate samples were taken at each station. Pre-combusted (550 ℃ for 4 h) 250 mL borosilicate glass bottles were rinsed three times with the sample seawater before being filled from the bottom, allowing it to overflow for approximately twice the time needed to fill the bottle to the top. Bottles were capped and left in the room for about 30 min (to bring cold deep-water samples to near room temperature). Then, 1 mL of water was extracted from each bottle to allow thermal expansion, and 50 μL of saturated $HgCl_2$ solution was added to poison biological activities. Sample bottles were sealed with Apiezon-L grease, and stoppers were fixed with rubber bands and clips. The samples were stored at room temperature for at least 24 h before onboard analysis or in coolers for transporting back to the home laboratory. Underway samples for DIC concentrations and δ^{13}C-DIC analyses were collected every 2 h from the ship's flow-through system during transits between stations. The samples were stored at room temperature for 2–3 h, and no $HgCl_2$ was added before onboard analysis.

Experimental setup

A G2131-i Isotope and Gas Concentration CRDS Analyzer (Picarro, USA) was employed along with an AS-D1 δ^{13}C-DIC Analyzer (Apollo SciTech, USA) for sample injection, CO_2 extraction, instrument control, and data acquisition in simultaneous DIC concentration and δ^{13}C-DIC measurements. This system and its accessories took up < 2 m of laboratory bench space (Figure 1).

The whole system is comprised of four components: (a) sample injection module, (b) CO_2 extraction module, (c) detection module, and (d) data processing and control module (Figure 2), similar to a previously described system (Deng et al. 2022; Su et al. 2019). The analytical procedure began with drawing 0.7 mL of phosphoric acid brine (2 % vol./vol. H_3PO_4 with 7 % wt./vol. NaCl) into a 10 mL syringe by the Cavro® XLP 6000 digital syringe pump (Precision ≤ 0.05 %, Tecan, USA) coupled to a 12-port valve and followed up by injection of the acid brine into the reactor. This step also cleaned residues from the previous cycle. While this pre-acid was bubbled in the reactor with a CO_2-free air stream, an additional 0.9 mL of the acid brine was drawn into the syringe, followed by a 6.5 mL sample (or standard). The excess of acid brine ensured that all DIC in the sample could completely convert to CO_2. Note the sample volume has been increased from our previous practice of 3.0–3.5 mL (Su et al. 2019). This larger volume ensured the CO_2 concentration remained within the instrument's optimal detection range for longer time, thus leading to more precise $\delta^{13}C$ measurements. Once a stable baseline of near zero CO_2 was reached in the reactor and the CO_2 detector, the sample and acid brine in the syringe were injected into the reactor at a controlled low speed to allow the acid brine to clear the sample DIC attached to the syringe wall into the reactor, where all carbonate species were converted to CO_2. The CO_2 was extracted and carried to the CRDS analyzer at a rate of 60 mL min^{-1} by CO_2-free compressed air from a 40 L cylinder, sufficient for 20 days of continuous analysis for approximately 700 samples. A preceding condenser was used to minimize water vapor interference (Pohlman et al. 2021). The CRDS concurrently reported CO_2 concentration ($^{12}CO_2$ + $^{13}CO_2$) and $\delta^{13}C$-CO_2 values at 1 Hz for about 500 s, with data similarly captured by the AS-D1's data processing and control module. The analytical cycle would complete when CO_2 levels drop below a set threshold (i.e., the deviation between 15 successive data points of CO_2 reading was

less than 5 ppm above the initial baseline), followed by a 120 s purge with carrier gas before the next cycle. Measurements occur under room temperature (20 ± 1 °C), each lasting about 13 min. The timeline of the entire analytical process is detailed in Table S1.

Calibrations and corrections

To determine the DIC concentration, we calculated the net CO_2 integration area by integrating the CO_2 concentration increase above baseline over time. A least square fitted line was developed to correlate net integration area with DIC mole amounts. This calibration covered a DIC concentration range of 1700 to 2300 μmol L^{-1}, using daily measurements of three volumes (5.5, 6.5, and 7.5 mL) of either in-house standard SB-1 or CRM. The density determined from recorded temperature and salinity measured in situ by the SBE 9plus CTD (accuracy ≤ 0.003 PSU, Seabird Scientific, USA) allowed for converting volume-based DIC concentrations to μmol kg^{-1}.

The δ^{13}C-CO_2 value of the DIC was simultaneously assessed. However, the Picarro G2131-i exhibited significant noise at low CO_2 concentrations (Figure 2e), as indicated by the manufacturer, with precision for δ^{13}C under 0.1 ‰ above 380 ppm CO_2 and 0.05 ‰ above 1000 ppm CO_2. To reduce noise, we applied a 400 ppm CO_2 cutoff. The CO_2 concentration-weighted mean δ^{13}C-CO_2 ($\delta^{13}C_{mean}$) for each analysis was calculated using eq 1, incorporating both raw δ^{13}C-CO_2 ($\delta^{13}C_{raw}$) data and net CO_2 concentration (CO_{2net}) readings from the CRDS at every time point.

$$\delta^{13}C_{mean} = \frac{\sum CO_{2net} \times \delta^{13}C_{raw}}{\sum CO_{2net}} \ (CO_{2net} > 400 \text{ ppm}) \qquad (1)$$

Due to the logistical complexities of implementing standard gas setups on a ship, we did not adopt the built-in δ^{13}C-CO_2 calibration program of the G2131-i CRDS system. Instead, leveraging multiple in-house standards with pre-calibrated δ^{13}C-DIC values facilitated the

correction of $\delta^{13}C_{mean}$ inaccuracies. To balance the need for frequent calibrations with the onboard sample processing efficiency, a calibration using one of the three in-house standards was conducted following analysis of every eight seawater samples. This procedure, detailed in Table S2, ensured each standard was assessed a minimum of three times daily. The $\delta^{13}C_{mean}$ values for each in-house standard, derived from its adjacent measurements, were used in a time-based linear regression model (eq 2) to track the instrumental drift and estimate the value of the standard's $\delta^{13}C$ signal ($\delta^{13}C_{est}$) at the time of each sample measurement. This enabled the establishment of a separate three-point calibration curve ($R^2 > 0.999$) for each measurement, incorporating the $\delta^{13}C_{est}$ and the exact $\delta^{13}C$-DIC values of three in-house standards.

$$\delta^{13}C_{est}(t) = \frac{\delta^{13}C_{mean}(t_1) - \delta^{13}C_{mean}(t_0)}{t_1 - t_0} \times (t - t_0) + \delta^{13}C_{mean}(t_0) \quad (2)$$

In our approach, each sample or reference material was subjected to a minimum of two and up to four consecutive measurements to achieve the preset relative standard deviation (RSD) of 0.001 for the net integration area and 0.06 for the CO_2-weighted mean of $\delta^{13}C$-CO_2. From these measurements, we selected two "valid" rounds that met our precision criteria, and the final DIC concentrations and $\delta^{13}C$-DIC results were always reported as an average of these two valid rounds. In addition, CRM Batch #188 and #195 were randomly included in the sample sequence as quality checks for DIC concentrations and $\delta^{13}C$-DIC analysis.

Field work

During the East Coast Ocean Acidification Cruise aboard NOAA Ship Ronald H. Brown in the summer of 2022 (ECOA 2022), the performance of our DIC and $\delta^{13}C$-DIC analytical system was extensively evaluated. The cruise, initially surveyed the Gulf of Maine and the Mid-Atlantic Bight (Leg 1), followed by a survey of the South Atlantic Bight (Leg 2). Over 40 days, we collected 1972 discrete CTD samples, including 186 duplicates from 228 water column stations,

plus 126 samples from the ship's underway water supply line (Figure 3). Of these, 1666 samples were analyzed onboard, supported by 480 measurements of in-house standards and CRMs to validate our method, while the rest were analyzed ashore within a month.

Assessment and discussion

Stability of in-house standards

While we could periodically calibrate the in-house DIC standards using the CRM when on board, the accuracy of δ^{13}C-DIC analyses primarily relied on the stability of our three in-house standards throughout the cruise as no CRM for δ^{13}C-DIC is available to our community. Therefore, the stability of our in-house standards plays a critical role in ensuring the accuracy and consistency of both DIC and δ^{13}C-DIC analyses, particularly on extended cruises, and needs to be evaluated before overall uncertainty estimation.

Figure 4 demonstrates the exceptional consistency of the δ^{13}C-DIC values of our in-house standards, as verified by IRMS over two months of onboard and post-cruise use, with average δ^{13}C-DIC values of –0.95 ± 0.02 ‰ for SB-1, –4.20 ± 0.03 ‰ for SB-2, and 1.09 ± 0.02 ‰ for SB-3 (n = 6). Moreover, these values closely aligned with their preparation sources (–0.99 ‰ for solid SB-1, –4.19 ‰ for solid SB-2, and 1.12 ‰ expected for SB-3). These validated average δ^{13}C-DIC values hence served as our calibration references.

This proven stability affirms our preparation and preservation method for in-house standards as effective for long-term δ^{13}C-DIC seawater analysis. The depletion of solutions in aluminum-coated bags to about one-sixth of their original volume did not notably alter the δ^{13}C-DIC. The method's adaptability in creating reference materials with precise δ^{13}C-DIC values enriches its utility across varied aquatic environments. While our findings advocate for theoretical or expected values' reliability in calibration, further experimental validations and

broader analytical method comparisons remain essential for affirming these standards' uniform stability and consistency across different laboratories.

Overall uncertainty of the method

The uncertainties for DIC concentration and δ^{13}C-DIC measurements stemmed from three main sources: standard material variations, determination processes, and repeated measurement variabilities. Figure 5 shows these uncertainties, with detailed calculations in Appendices S2 and S3.

We especially evaluated the uncertainty of repeated measurements by successively measuring eight replicate seawater samples sequentially drawn from one Niskin bottle at 226 m depth and processed identically. Analyzed in random order (3, 1, 6, 5, 2, 4, 7, 8), a discernible increase in δ^{13}C-DIC was noted from the sixth sample onwards (Figure 6). The average δ^{13}C-DIC was 0.34 ± 0.01 ‰ (1σ) for the first five samples and 0.40 ± 0.01 ‰ for the last three samples, suggesting potential ^{13}C-DIC gas exchange with headspace air when only half the volume of seawater was left in the Niskin bottle. During the sampling process, δ^{13}C-DIC samples were collected after DO, pH, and DIC samples for NOAA lab analysis, with about 1 L of water used per δ^{13}C-DIC bottle. Each sample type typically required ~ 2 min to collect (doubling for replicates), resulting in a total elapsed time of 8–10 min from the Niskin bottle's initial opening to δ^{13}C-DIC sampling. The difference in DIC concentrations among the eight samples was not significant, with the first five samples having an average DIC concentration of 2174.3 ± 0.5 μmol kg^{-1} and the average DIC concentration of the last three samples being 2174.6 ± 0.3 μmol kg^{-1}. We excluded the last three (No. 6, 7, 8) to eliminate potential sampling bias and reported a standard deviation of 0.8 μmol kg^{-1} (RSD = 0.04 %) for DIC concentrations and 0.017 ‰ for δ^{13}C-DIC of the ten repeated analyses of the first five duplicates, as each was measured twice. In

our approach, the DIC concentrations and δ^{13}C-DIC results are always reported as an average of two repeatable analyses; thus, the standard uncertainty of the repeated measurements was 0.6 μmol kg^{-1} (RSD = 0.03 %) for DIC concentrations and 0.012 ‰ for δ^{13}C-DIC. This reflects the residual effects of random errors in sampling, handling, and instrumental drift after calibration and correction procedures are applied.

To conclude, the relative combined standard uncertainty of DIC concentration was 0.06 % (1σ), or 1.2 μmol kg^{-1} at a DIC concentration of ~ 2000 μmol kg^{-1}. Meanwhile, the combined standard uncertainty for the onboard measurement of δ^{13}C-DIC was 0.03 ‰ (1σ). These uncertainties satisfy not only the recommended precisions of GOOS but also compare favorably to conventional methods. For instance, the coulometry method with Single-Operator Multiparameter Metabolic Analyzer (SOMMA) and the non-dispersive infrared absorption (NDIR) method report uncertainties for DIC concentrations between 1.19 to 1.65 μmol kg^{-1} (Johnson 1992; Johnson et al. 1985; Johnson et al. 1999; Johnson et al. 1987) and 2 μmol kg^{-1} (Huang et al. 2012), respectively, while the best-reported uncertainty for δ^{13}C-DIC via IRMS is about 0.03 ‰ based on a 100 mL sample (Quay et al. 2007; Quay et al. 2003), with other laboratories often reporting around 0.1 ‰ based on smaller sample volume of 1–2 mL (Cheng et al. 2019). We suggest that the methodologies employed in our study are as precise as existing techniques, validating the reliability of the onboard measurements.

Evaluation of onboard analytical performance

Repeatability

The ECOA 2022 cruise analyzed 186 replicate samples from 228 CTD stations, covering depths from the sea surface to 4600 m. The DIC concentrations of these samples ranged between 1900 and 2250 μmol kg^{-1}, and the δ^{13}C-DIC values varied from –0.5 ‰ to 1.8 ‰. Excluding four

pairs of abnormal data with a DIC concentration difference greater than 10 μmol kg^{-1} and δ^{13}C-DIC difference greater than 0.2 ‰, the mean absolute differences were 1.6 ± 1.5 μmol kg^{-1} for DIC and 0.05 ± 0.04 ‰ for δ^{13}C-DIC (1σ, n = 182), both within 2σ of the overall uncertainties of the method.

Moreover, repeatability in measuring DIC concentration and δ^{13}C-DIC across coastal samples remained consistent, unaffected by the sample's DIC concentration (Figure 7). Injecting 6.5 mL of seawater with a minimum DIC concentration of 1900 μmol kg^{-1} produced peak CO_2 signal between 2600–3000 ppm and sustained concentrations above 2000 ppm for at least 90 s, above 1000 ppm for 120 s, and above 400 ppm for 150 s (data not presented). The high CO_2 concentration with an extended duration is sufficient and critical to secure a stable CO_2-weighted mean of δ^{13}C-CO_2 for accurate δ^{13}C-DIC determination, with a 400-ppm CO_2 concentration cutoff. To achieve this, we have nearly doubled sample volume from our previous practice (Deng et al. 2022; Su et al. 2019). Furthermore, comparisons between onboard and shore-based measurements of 136 onboard and 46 shore-based pairs revealed consistent performance. Onboard samples showed a mean absolute difference of 1.5 ± 1.4 μmol kg^{-1} for DIC and 0.05 ± 0.04 ‰ for δ^{13}C-DIC, while shore-based analyses had similar discrepancies, 1.8 ± 1.8 μmol kg^{-1} for DIC concentration and 0.04 ± 0.04 ‰ for δ^{13}C-DIC, confirming the method's reliability.

Accuracy evaluation

For method validation, we utilized CRMs. Our in-house standards SB-1, SB-2, and SB-3 were initially calibrated using CRMs from Batches #197 and #199. Throughout the cruise, we analyzed 43 bottles of CRMs as quality control samples: 36 from Batch #188 and 7 from Batch #195. The results of these analyses, including DIC concentration and δ^{13}C-DIC measurements, are summarized in Table 1.

Table 1. Summary of statistical properties for measured dissolved inorganic carbon (DIC) concentrations and stable isotopic composition of DIC (δ^{13}C-DIC) in certified reference materials (CRMs) from Batch #188 and #195.

	CRM #188		CRM #195	
	DIC (μmol kg^{-1})	δ^{13}C-DIC (‰)	DIC (μmol kg^{-1})	δ^{13}C-DIC (‰)
Average	2100.7	–0.20	2026.0	0.88
Standard deviation	1.7	0.04	1.1	0.03
Median	2101.1	–0.19	2026.2	0.88
Maximum	2103.2	–0.12	2027.3	0.93
Minimum	2096.0	–0.31	2024.8	0.84
n	36	36	7	7

Note: The certified DIC concentrations for CRM Batch #188 and #195 are 2099.26 ± 0.52 μmol kg^{-1} and 2024.96 ± 0.52 μmol kg^{-1}, respectively.

We evaluated the bias in DIC measurements by comparing our results (Figure 8a) with the certified values of CRMs, finding average discrepancies of 1.4 ± 1.7 μmol kg^{-1} for CRM #188 and 1.0 ± 1.1 μmol kg^{-1} for CRM #195. Statistical analysis through two one-tailed *t*-tests, at a 99.5 % confidence interval, yielded *p*-values less than 0.001, demonstrating that our measured DIC concentrations were statistically higher than the certified values for both CRM batches. The observed discrepancy in DIC measurements was linked to temperature fluctuations of in-house standards affecting their density. The aluminum bags holding the standards were hung near an AC vent on the ceiling, likely causing their temperatures to diverge from recorded values as the thermometer was placed close to the sample bottles. This situation, evidenced by a hypothetical 2 °C standard temperature deviation altering measured DIC concentration by ~ 1 μmol kg^{-1},

remained within the GOOS's ± 2 μmol kg^{-1} accuracy range, hence no adjustments were made in the current study. Future measures will include attaching thermometers directly to the standard bags or repositioning them away from AC influences to ensure consistent temperature management.

The accuracy of δ^{13}C-DIC analysis and the stability of the analyzer were first examined by directly comparing CRDS with IRMS measurements on the CRM from Batch #188. Duplicate IRMS analysis at the University of California Davis Stable Isotope Facility of an unopened CRM bottle provided a reference δ^{13}C-DIC value of –0.19 ± 0.02 ‰. Our CRDS-based method against in-house standards produced an average δ^{13}C-DIC value of –0.20 ± 0.04 ‰ with a median of –0.19 ‰ across 36 CRM bottles. This close agreement with the IRMS results corroborates our analytical system's precision and matches or surpasses previously documented accuracies, varying from 0.03 ‰ to 0.23 ‰ across different methodologies (Bass et al. 2012; Cheng et al. 2019; Su et al. 2019). The standard deviation was 0.04 ‰ for δ^{13}C-DIC measurements of 36 CRM bottles from Batch #188 throughout the cruise, indicating high stability for long-term onboard isotopic analyses. Enhanced measurement consistency was achieved through a time-based linear regression calibration and correction model, significantly reducing δ^{13}C-DIC variability compared to uncorrected results, which had a higher standard deviation of 0.13 ‰ (Figure 8b).

The minimal standard deviations for δ^{13}C-DIC of CRM Batches #188 (0.04 ‰) and #195 (0.03 ‰) underscore their reliability as consistent liquid standards for δ^{13}C-DIC analyses in seawater. A previous work by Cheng et al. (2019) also revealed a considerable narrowing of measurement variations from 0.10 ‰ to 0.06 ‰ in an international intercomparison study after applying CRM for interlaboratory correction . A key advantage to adopting CRM as a δ^{13}C-DIC

reference material lies in its wide availability within the marine carbonate chemistry community. If the δ^{13}C-DIC of CRM from a subset of batches can be certified before distribution, the δ^{13}C measurement community could calibrate their secondary in-house standard using the CRM, thus increasing the interlaboratory consistency. This approach positions CRM as a comprehensive standard for DIC concentration and δ^{13}C-DIC measurements, simplifying quality control protocols.

Interlaboratory reproducibility of DIC analysis

To assess inter-laboratory consistency, DIC concentrations measured by our CRDS method were compared with coulometry measurements by the National Oceanic and Atmospheric Administration (NOAA)'s Atlantic Oceanographic & Meteorological Laboratory (AOML), using 1723 samples analyzed by the SOMMA system during the same cruise (Johnson 1992; Johnson et al. 1985; Johnson et al. 1999; Johnson et al. 1987). After outlier detection using interquartile ranges (Rousseeuw and Hubert 2011), a satisfactory agreement was found (Figure 9), with an average difference of 2.4 ± 3.8 μmol kg^{-1} between CRDS and coulometry methods, indicating an acceptable accuracy range for onboard measurements. Compared to the discrepancy of onboard analyses (2.0 ± 3.8 μmol kg^{-1}, n = 1278), that of shore-based laboratory result (3.5 ± 3.7 μmol kg^{-1}, n = 386) was slightly higher ($p < 0.001$ at a 99.5 % confidence interval), suggesting that transportation and storage might impact DIC concentrations. The correlation coefficient of 0.298 between discrepancies and DIC concentrations demonstrated that our CRDS method is adequate for a wide range of DIC concentrations in oceanic and coastal waters.

δ^{13}C-DIC comparison with historical data

As there is no analysis of the same water with IRMS for comparison, we make a comparison with historical data at the offshore stations (Figure 10a), which had been occupied

during the World Ocean Circulation Experiment (WOCE) A22 cruise in 1997 (Transect 1) and the Global Ocean Ship-based Hydrographic Investigations Program (GO-SHIP) A22 cruises in 2021 and 2012 (Transect 2) (Olsen et al. 2020). During these cruises, δ^{13}C-DIC samples collected in 500 mL bottles were analyzed post-cruise at the National Ocean Sciences Accelerator Mass Spectrometry Facility, with a replication of ± 0.03 ‰ (McNichol et al. 2010). In the offshore stations along both Transect 1 and Transect 2, we can observe the decrease of δ^{13}C-DIC over time in all water masses, that is 1997 (Figure 10c) over 2022 (Figure 10b) and 2012 (Figure 10f) over 2022 (Figure 10d) and 2021 (Figure 10e). This is particularly clear for the surface waters of the Gulf Stream (GS).

In our 2022 transects (Figure 11), surface δ^{13}C-DIC varied widely (0.64–1.56 ‰), inversely correlating with DIC concentrations due to photosynthesis. Phytoplankton preference for ^{12}C during photosynthesis leads to ^{13}C-enriched DIC in surface waters (Ge et al. 2022). Below the surface mixed layer, the δ^{13}C-DIC minimum (0.28–0.46 ‰) at 70–200 m reflected organic matter remineralization. Concurrently, the DIC concentration peaked at about 2200 μmol kg^{-1} in the oxygen minimum zone (200–400 m). The observed mismatch between the minimum δ^{13}C-DIC at shallower depths and the maximum DIC concentration may result from two primary processes. Firstly, atmospheric CO_2 Suess effect (that is δ^{13}C-CO_2 becomes more negative with time) and its invasion into the ocean introduced a progressively lighter δ^{13}C-CO_2 signal, which affects the upper ocean δ^{13}C-DIC relatively more substantially than the DIC concentration increase. Secondly, mixing colder, low-oxygen Antarctic Intermediate Water and other intermediate waters (AAIW+) with warmer Gulf Stream (GS) water shifts δ^{13}C-DIC values positive below 100 m. This is because AAIW+, when formed at colder surface temperatures, had

a more positive δ^{13}C-DIC signal due to enhanced isotope fractionation during air-sea equilibrium (Broecker and Maier-Reimer 1992; Quay et al. 2017).

In the deep ocean, the δ^{13}C-DIC increased with depth, stabilizing around 0.97 ‰ at 2000 m due to mixing with the upper layer of the North Atlantic Deep Water (uNADW), while DIC concentration slightly dropped to around 2170 μmol kg^{-1}. Given the expectation that δ^{13}C-DIC in deep ocean seawater remains stable over centuries, unaffected by anthropogenic carbon uptake (Cheng et al. 2019), we compared our 2022 measurements at depths beyond 2000 meters with historical data from similar locations during the 1997 WOCE A22 and the 2012 and 2021 GO-SHIP A22 cruises. Our findings reveal an average δ^{13}C-DIC value of 0.97 ± 0.03 ‰ (1σ, n = 15), closely matching historical average of 1.00 ± 0.04 ‰ (1σ, n = 27), further affirming the accuracy of our CRDS δ^{13}C-DIC analytical approach.

In addition, the observed δ^{13}C-DIC variations in the upper ocean point towards changes in biogeochemical processes or the impact of the Suess effect due to anthropogenic CO_2 uptake (Quay et al. 2017). Our analysis shows a marked decrease in δ^{13}C-DIC over the decades (Figure 10 and 11), especially within the mixed layer, progressively lessening with depth to around 1500 meters (–0.006 ‰ yr^{-1}). This decrease underscores the increased influence of anthropogenic carbon in shallower waters. For depth profiles taken at the two transects in 2022, the average δ^{13}C-DIC values observed were 0.50 ± 0.16 ‰ for the Gulf Stream water, 0.49 ± 0.07 ‰ for the AAIW+, and 0.77 ± 0.06 ‰ for the uNADW. At stations along Transect 1, the δ^{13}C-DIC values experienced a decrease of about 0.27 ‰ in the Gulf Stream water, 0.26 ‰ in the AAIW+, and 0.08 ‰ in the uNADW, while the corresponding DIC concentration increased by 1.0 μmol kg^{-1}, 14.8 μmol kg^{-1} and 13.0 μmol kg^{-1}, respectively, in these water masses over the past 25 years. At stations along Transect 2, the δ^{13}C-DIC between 2022 and 2012 decreased by 0.50 ‰ in the Gulf

Stream water, 0.10 ‰ in the AAIW+, and 0.10 ‰ in the uNADW, while the DIC concentration increase over the past decade were 29.9 μmol kg^{-1}, 14.3 μmol kg^{-1}, and 12.0 μmol kg^{-1}, respectively. Compared to the decadal changes in DIC concentration (6–12 μmol kg^{-1}), the decadal changes in δ^{13}C-DIC (–0.1 ‰) are more distinguishable from seasonal variations (± 0.2 ‰ for δ^{13}C-DIC and ± 30 μmol kg^{-1} for DIC concentration) and vertical trends (0.4–1.2 ‰ for δ^{13}C-DIC and 160–240 μmol kg^{-1} for DIC concentration) (Gruber et al. 2002), thus making the δ^{13}C-DIC signal potentially a more sensitive tool for detecting anthropogenic CO_2 accumulation. Given the uncertainty of 1.2 μmol kg^{-1} for DIC concentration and 0.03 ‰ for δ^{13}C-DIC value, both parameters from our measurements are sufficient for studying their decadal variabilities in the ocean. A combined use of both datasets would provide a powerful approach for constraining anthropogenic CO_2 in the ocean.

Comments and recommendations

The CRDS-based analyzer streamlines δ^{13}C-DIC analysis with its operational efficiency and simplicity, marking an advancement over traditional IRMS methods that require lengthy onshore processing and headspace equilibration. Using the CO_2 extraction device, our method enables immediate seawater analysis post-collection. The system's automated functionality based on a 12-valve pump supports loading up to 6 samples at one time and unattended operation for over 3 h. We are also evaluating an enhanced system featuring a 24-valve pump, which allows the operator to load up to 18 samples each time and unattended operation for more than 12 h. This improvement further reduces the workload, making it feasible for a single operator to perform DIC/δ^{13}C-DIC analysis during typical 12-h sea shifts.

During the first leg of the ECOA 2022, we employed a single analytical system (Unit #1), later doubling our capacity by introducing Unit #2 for the second leg. Across 40 days, Unit #1

processed 1220 samples, while Unit #2 analyzed 446 during the latter half. This efficiency contrasts with historical data collection rates; over three decades, only 6820 δ^{13}C-DIC results have been gathered from 32 Atlantic Ocean cruises, averaging 213 δ^{13}C-DIC values per cruise (Becker et al. 2016). More recently, the 2010 GO-SHIP A13.5 cruise collected merely 634 δ^{13}C-DIC data compared to 3009 DIC data. By utilizing two analyzers capable of processing 30 samples daily each, we could nearly match the sample density of DIC concentration measurements during a 50-day GO-SHIP cruise, allowing for comprehensive onboard analysis. This approach was validated during the 2023 A16N expedition, where nearly 3000 samples were analyzed directly onboard by two Cai Laboratory members from the University of Delaware, underscoring the significant advancements in our analytical capacity.

The deployment of the CRDS-based analyzer during the ECOA 2022 cruise enabled the collection of a substantial δ^{13}C-DIC dataset along North America's eastern ocean margins. This comprehensive dataset, combined with DIC concentration and total alkalinity measurements, offers enhanced capacity in assessing anthropogenic carbon changes through advanced regression and back-calculation methods (Friis et al. 2005; Körtzinger et al. 2003). Additionally, it allows for detailed evaluations of DIC and δ^{13}C-DIC variations against conservative mixing models in coastal areas, shedding light on the impact of various biogeochemical processes and carbon sources on the DIC pool (Burt et al. 2016; Deng et al. 2022; Su et al. 2020).

Moreover, diverse and intricate coastal regions are critical interfaces for carbon flux and transformation between terrestrial ecosystems and the open ocean, making high-spatial-resolution δ^{13}C-DIC datasets critically needed for resolving unanswered key geochemical and environmental questions. For example, in a recent coupled physical and biogeochemical model study, Kwon et al. (2021) suggested that lateral transport of ^{13}C depleted organic and inorganic

carbon from land (river and groundwater) to the ocean was markedly underestimated in the current global carbon cycle and flux models. According to their model simulations, without this territorial export, the deep ocean δ^{13}C-DIC value would be 0.2–0.3 ‰ higher. A key geochemical nature that allows this mechanism to work lies in the fact that while most of the proposed enhanced carbon export can be returned to the atmosphere as CO_2 in the coastal zone in a timescale of about one year, the ^{13}C-DIC is exported to the open ocean as the air-sea change of ^{13}C-CO_2 has a much longer timescale of nearly a decade. High-quality and high-spatial-resolution δ^{13}C-DIC datasets in ocean margins, such as those we collected along the North American ocean margins during ECOA 2022, provide essential information for validating and improving these important model predictions. As more δ^{13}C-DIC data becomes available in coastal and open oceans as a result of the availability of our high throughput and seagoing analytical method, our understanding of the terrestrial-to-oceanic carbon flux and the dynamics of anthropogenic CO_2 accumulation in the ocean will be improved rapidly in future studies.

Supporting Information

Additional information regarding the calculation of the mixing ratio between ^{13}C labeled and ordinary $NaHCO_3$ for the in-house standard with δ^{13}C-DIC > 0 ‰ (Appendix S1), the calculation of the combined relative standard uncertainty for the DIC concentration (Appendix S2) and the combined standard uncertainty for the δ^{13}C-DIC measurements (Appendix S3), the timeline of the entire analytical process (Table S1), and an example of a daily analysis cycle (Table S2).

Acknowledgments

This work was supported by the National Science Foundation (NSF) award OCE-2123768, the NOAA's Ocean Acidification Program (OAP) (award # NA21NOS0120096), and the

Delaware Bioscience Center for Advanced Technology (CAT) program (award # 12A00448). XL would be thankful to the support from the Cooperative Institute for Climate, Ocean, & Ecosystem Studies (CICOES) under NOAA Cooperative Agreement NA20OAR4320271, Contribution No. 2024-1388.

References

Atekwana, E. A., and R. V. Krishnamurthy. 1998. Seasonal variations of dissolved inorganic carbon and $\delta^{13}C$ of surface waters: application of a modified gas evolution technique. Journal of Hydrology **205:** 265-278.

Bass, A. M., M. I. Bird, N. C. Munksgaard, and C. M. Wurster. 2012. ISO-CADICA: Isotopic – continuous, automated dissolved inorganic carbon analyser. Rapid Communications in Mass Spectrometry **26:** 639-644.

Bauer, J. E., E. R. M. Druffel, D. M. Wolgast, and S. Griffin. 2001. Sources and cycling of dissolved and particulate organic radiocarbon in the Northwest Atlantic Continental Margin. Global Biogeochemical Cycles **15:** 615-636.

Becker, M., N. Andersen, H. Erlenkeuser, M. P. Humphreys, T. Tanhua, and A. Körtzinger. 2016. An internally consistent dataset of $\delta^{13}C$-DIC in the North Atlantic Ocean – NAC13v1. Earth System Science Data **8:** 559-570.

Becker, M. and others 2012. Using cavity ringdown spectroscopy for continuous monitoring of $\delta^{13}C(CO_2)$ and fCO_2 in the surface ocean. Limnology and Oceanography: Methods **10:** 752-766.

Broecker, W. S., and E. Maier-Reimer. 1992. The influence of air and sea exchange on the carbon isotope distribution in the sea. Global Biogeochemical Cycles **6:** 315-320.

Burt, W. J. and others 2016. Carbon sources in the North Sea evaluated by means of radium and stable carbon isotope tracers. Limnology and Oceanography **61:** 666-683.

Call, M., K. G. Schulz, M. C. Carvalho, I. R. Santos, and D. T. Maher. 2017. Technical note: Coupling infrared gas analysis and cavity ring down spectroscopy for autonomous, high-temporal-resolution measurements of DIC and $\delta^{13}C$–DIC. Biogeosciences **14:** 1305-1313.

Carter, B. R. and others 2019. Pacific anthropogenic carbon between 1991 and 2017. Global Biogeochemical Cycles **33:** 597-617.

Cheng, L. and others 2019. An international intercomparison of stable carbon isotope composition measurements of dissolved inorganic carbon in seawater. Limnology and Oceanography: Methods **17:** 200-209.

Deng, X., Q. Li, J. Su, C.-Y. Liu, E. Atekwana, and W.-J. Cai. 2022. Performance evaluations and applications of a δ^{13}C-DIC analyzer in seawater and estuarine waters. Science of The Total Environment **833:** 155013.

Dickson, A. G., C. L. Sabine, J. R. Christian, and Eds. 2007. Guide to Best Practices for Ocean CO_2 Measurements. North Pacific Marine Science Organization.

Doney, S. C., V. J. Fabry, R. A. Feely, and J. A. Kleypas. 2009. Ocean acidification: The other CO_2 problem. Annual Review of Marine Science **1:** 169-192.

Friedlingstein, P. and others 2023. Global Carbon Budget 2023. Earth Syst. Sci. Data **15:** 5301-5369.

Friis, K., A. Körtzinger, J. Pätsch, and D. W. R. Wallace. 2005. On the temporal increase of anthropogenic CO_2 in the subpolar North Atlantic. Deep Sea Research Part I: Oceanographic Research Papers **52:** 681-698.

Ge, T. and others 2022. Stable carbon isotopes of dissolved inorganic carbon in the Western North Pacific Ocean: Proxy for water mixing and dynamics. Frontiers in Marine Science **9:** 998437.

Gruber, N., C. Keeling, and N. Bates. 2002. Interannual variability in the North Atlantic Ocean carbon sink. Science (New York, N.Y.) **298:** 2374-2378.

Huang, W.-J., Y. Wang, and W.-J. Cai. 2012. Assessment of sample storage techniques for total

alkalinity and dissolved inorganic carbon in seawater. Limnology and Oceanography: Methods **10:** 711-717.

Humphreys, M. P., E. P. Achterberg, A. M. Griffiths, A. McDonald, and A. J. Boyce. 2015. Measurements of the stable carbon isotope composition of dissolved inorganic carbon in the northeastern Atlantic and Nordic Seas during summer 2012. Earth System Science Data **7:** 127-135.

Johnson, K. M. 1992. Single-operator multiparameter metabolic analyzer (SOMMA) for total carbon dioxide (C_T) with coulometric detection. Brookhaven National Laboratory.

Johnson, K. M., A. E. King, and J. M. Sieburth. 1985. Coulometric TCO_2 analyses for marine studies: An introduction. Marine Chemistry **16:** 61-82.

Johnson, K. M., A. Körtzinger, L. Mintrop, J. C. Duinker, and D. W. R. Wallace. 1999. Coulometric total carbon dioxide analysis for marine studies: measurement and internal consistency of underway TCO_2 concentrations. Marine Chemistry **67:** 123-144.

Johnson, K. M., J. M. Sieburth, P. J. l. Williams, and L. Brändström. 1987. Coulometric total carbon dioxide analysis for marine studies: Automation and calibration. Marine Chemistry **21:** 117-133.

Keeling, C. D. 1979. The Suess effect: ^{13}Carbon-^{14}Carbon interrelations. Environment International **2:** 229-300.

Körtzinger, A., P. D. Quay, and R. E. Sonnerup. 2003. Relationship between anthropogenic CO_2 and the ^{13}C Suess effect in the North Atlantic Ocean. Global Biogeochemical Cycles **17:** 5-1-5-20.

Kwon, E. Y., T. DeVries, E. D. Galbraith, J. Hwang, G. Kim, and A. Timmermann. 2021. Stable carbon isotopes suggest large terrestrial carbon inputs to the global ocean. Global

Biogeochemical Cycles **35:** e2020GB006684.

Le Quéré, C. and others 2009. Trends in the sources and sinks of carbon dioxide. Nature Geoscience **2:** 831-836.

Lynch-Stieglitz, J., T. F. Stocker, W. S. Broecker, and R. G. Fairbanks. 1995. The influence of air-sea exchange on the isotopic composition of oceanic carbon: Observations and modeling. Global Biogeochemical Cycles **9:** 653-665.

McNichol, A. P., P. D. Quay, A. R. Gagnon, and J. R. Burton. 2010. Collection and Measurement of Carbon Isotopes in Seawater DIC, p. 12. *In* E. M. Hood, C. L. Sabine, B. M. Sloyan and eds [eds.], The GO-SHIP Repeat Hydrography Manual: A Collection of Expert Reports and Guidelines. Version 1.

Olack, G. A., A. S. Colman, C. A. Pfister, and J. T. Wootton. 2018. Seawater DIC analysis: The effects of blanks and long-term storage on measurements of concentration and stable isotope composition. Limnology and Oceanography: Methods **16:** 160-179.

Olsen, A. and others 2020. An updated version of the global interior ocean biogeochemical data product, GLODAPv2.2020. Earth Syst. Sci. Data **12:** 3653-3678.

Pohlman, J. W., M. Casso, C. Magen, and E. Bergeron. 2021. Discrete sample introduction module for quantitative and isotopic analysis of methane and other gases by cavity ring-down spectroscopy. Environmental Science & Technology **55:** 12066-12074.

Quay, P., R. Sonnerup, D. Munro, and C. Sweeney. 2017. Anthropogenic CO_2 accumulation and uptake rates in the Pacific Ocean based on changes in the $^{13}C/^{12}C$ of dissolved inorganic carbon. Global Biogeochemical Cycles **31:** 59-80.

Quay, P. and others 2007. Anthropogenic CO_2 accumulation rates in the North Atlantic Ocean from changes in the $^{13}C/^{12}C$ of dissolved inorganic carbon. Global Biogeochemical Cycles **21:**

GB1009.

Quay, P., R. Sonnerup, T. Westby, J. Stutsman, and A. McNichol. 2003. Changes in the $^{13}C/^{12}C$ of dissolved inorganic carbon in the ocean as a tracer of anthropogenic CO_2 uptake. Global Biogeochemical Cycles **17:** 4-1-4-20.

Quay, P. D., J. Stutsman, R. A. Feely, and L. W. Juranek. 2009. Net community production rates across the subtropical and equatorial Pacific Ocean estimated from air-sea $\delta^{13}C$ disequilibrium. Global Biogeochemical Cycles **23:** GB2006.

Rousseeuw, P. J., and M. Hubert. 2011. Robust statistics for outlier detection. WIREs Data Mining and Knowledge Discovery **1:** 73-79.

Samanta, S., T. K. Dalai, J. K. Pattanaik, S. K. Rai, and A. Mazumdar. 2015. Dissolved inorganic carbon (DIC) and its $\delta^{13}C$ in the Ganga (Hooghly) River estuary, India: Evidence of DIC generation via organic carbon degradation and carbonate dissolution. Geochim Cosmochim Ac **165:** 226-248.

Sonnerup, R. E., and P. D. Quay. 2012. ^{13}C constraints on ocean carbon cycle models. Global Biogeochemical Cycles **26**.

Su, J. and others 2020. Source partitioning of oxygen-consuming organic matter in the hypoxic zone of the Chesapeake Bay. Limnology and Oceanography **65:** 1801-1817.

Su, J., W.-J. Cai, N. Hussain, J. Brodeur, B. Chen, and K. Huang. 2019. Simultaneous determination of dissolved inorganic carbon (DIC) concentration and stable isotope ($\delta^{13}C$-DIC) by Cavity Ring-Down Spectroscopy: Application to study carbonate dynamics in the Chesapeake Bay. Marine Chemistry **215:** 103689.

Yang, B., S. R. Emerson, and P. D. Quay. 2019. The subtropical ocean's biological carbon pump determined from O_2 and DIC/DI^{13}C tracers. Geophysical Research Letters **46:** 5361-5368.

Yang, X. and others 2018. Treated wastewater changes the export of dissolved inorganic carbon and its isotopic composition and leads to acidification in coastal oceans. Environmental Science & Technology **52:** 5590-5599.

Zhang, J., P. D. Quay, and D. O. Wilbur. 1995. Carbon isotope fractionation during gas-water exchange and dissolution of CO_2. Geochim Cosmochim Ac **59:** 107-114.

Figure legends

Figure 1. Photograph of the DIC/δ^{13}C-DIC analytical equipment installed onboard NOAA Ship Ronald H. Brown.

Figure 2. The schematic of the dissolved inorganic carbon (DIC) concentration and stable isotopic composition of DIC (δ^{13}C-DIC) analytical system is subdivided into four distinct modules: (a) the sample injection module, (b) the CO_2 extraction module, (c) the detection module, and (d) the data processing and control module; and (e) a typical output showing data collected for one measurement of CO_2 concentration and stable isotopic composition of CO_2 (δ^{13}C-CO_2). Solid lines represent the flow of liquid, while dashed lines denote the flow of gas.

Figure 3. Map showing the study area and sampling locations of the ECOA 2022 cruise. Transect 1 and Transect 2 show locations of selected deep-water stations with a water depth of > 2000 m for comparisons with historical data.

Figure 4. The stable isotopic composition of DIC (δ^{13}C-DIC) values measured by Isotope Ratio Mass Spectrometry (IRMS) for three in-house standards periodically subsampled at sea and after the cruise. The error bars indicate the standard deviation of δ^{13}C-DIC for in-house standards stored in different gas-tight bags. The dashed lines show the average δ^{13}C-DIC value for each in-house standard.

Figure 5. The sources of uncertainties for (a) the dissolved inorganic carbon (DIC) concentration and (b) the stable isotopic composition of DIC (δ^{13}C-DIC) measurements. Numbers in the brackets indicate the values of relative standard uncertainties for the DIC concentration and the standard uncertainties for the δ^{13}C-DIC from different parts of sources.

Figure 6. Dissolved inorganic carbon (DIC) concentrations and stable isotopic composition of DIC (δ^{13}C-DIC) values of eight duplicate seawater samples collected at a depth of 226 m. The two ends of the error bar indicate the results of two rounds of measurements, and the symbol indicates the mean value.

Figure 7. The absolute dissolved inorganic carbon (DIC) concentration differences (blue circles) and stable isotopic composition of DIC (δ^{13}C-DIC) differences (red triangles) against the DIC concentrations of discrete replicate samples collected during the cruise. 4 out of 186 pairs of duplicate measurements with a DIC concentration difference greater than 10 μmol kg^{-1} and δ^{13}C-DIC difference greater than 0.2 ‰ were excluded in advance.

Figure 8. Measured (a) DIC concentrations (filled circles) and (b) stable isotopic composition of DIC (δ^{13}C-DIC) values (filled triangles) of certified reference materials (CRMs) from Batch #188 relative to the analysis date (n = 36). The dashed lines show the average DIC and δ^{13}C-DIC values of CRM #188 measured during the 40-day onboard period. The empty triangles indicate raw δ^{13}C-DIC values derived from single-point calibration without employing a time-dependent linear regression method for correction, highlighting the long-term instrument drift.

Figure 9. Dissolved inorganic carbon (DIC) concentration results measured by Cavity Ring-Down Spectroscopy (CRDS) on board (blue circle) or on shore (red triangle) plotted against DIC concentrations obtained through onboard coulometry measurements conducted by National Oceanic and Atmospheric Administration (NOAA)'s Atlantic Oceanographic & Meteorological Laboratory (AOML).

Figure 10. (a) Locations of selected deep-water stations with a water depth of > 2000 m for comparison with historical data. These stations were occupied during the East Coast Ocean Acidification (ECOA) 2022 cruise (blue circles) and their nearby stations visited during the

World Ocean Circulation Experiment (WOCE) A22 cruise in 1997 (yellow circles) and the Global Ocean Ship-based Hydrographic Investigations Program (GO-SHIP) A22 cruises in 2021 and 2012 (red circles). The stable isotopic composition of DIC (δ^{13}C-DIC) overlay Temperature-Salinity (T-S) diagrams show the δ^{13}C-DIC of different water masses in full water columns at Transect 1 in (b) 2022 (ECOA 2022) and (c) 1997 (WOCE A22), and the δ^{13}C-DIC in different water masses at Transect 2 in (d) 2022 (ECOA 2022), (e) 2021 (GO-SHIP A22), and (f) 2012 (GO-SHIP A22). GS, AAIW+, and uNADW denote the Gulf Stream water, the Antarctic Intermediate Water and other intermediate waters, and the upper layer of the North Atlantic Deep Water, respectively.

Figure 11. (a) The dissolved inorganic carbon (DIC) concentration and stable isotopic composition of DIC (δ^{13}C-DIC) depth profiles measured during the East Coast Ocean Acidification (ECOA) 2022 cruise (circles) at Transect 1 compared to that measured during the World Ocean Circulation Experiment (WOCE) A22 cruise in 1997 (diamonds) at the same location. (b) The DIC and δ^{13}C-DIC depth profiles measured at Transect 2 during the ECOA 2022 cruise (circles) compared to that measured at the exact location in 2021 (triangles) and Station 9 in 2012 (squares) during the Global Ocean Ship-based Hydrographic Investigations Program (GO-SHIP) A22 cruises. Black arrows indicate the decrease of δ^{13}C-DIC over the past few years.

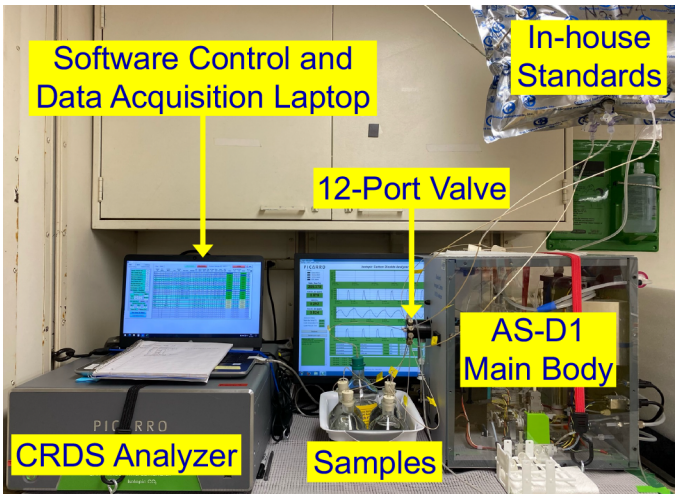

1.tif

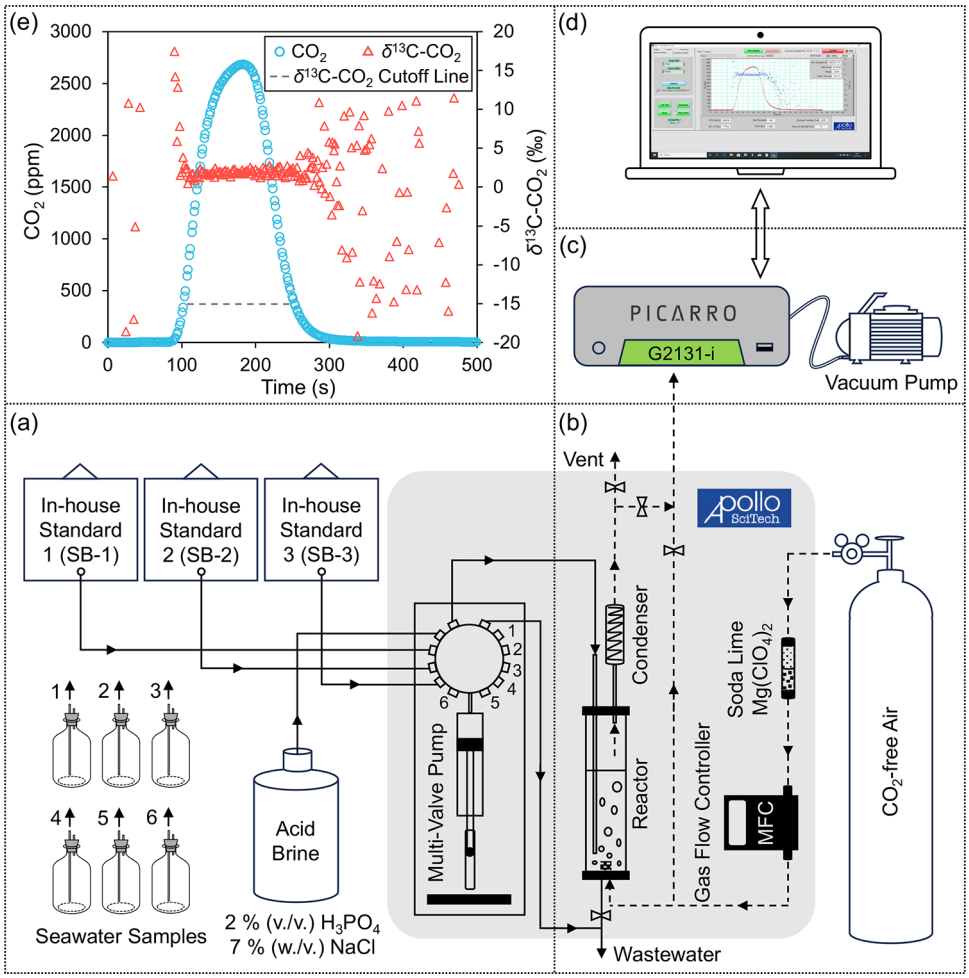

2.tif

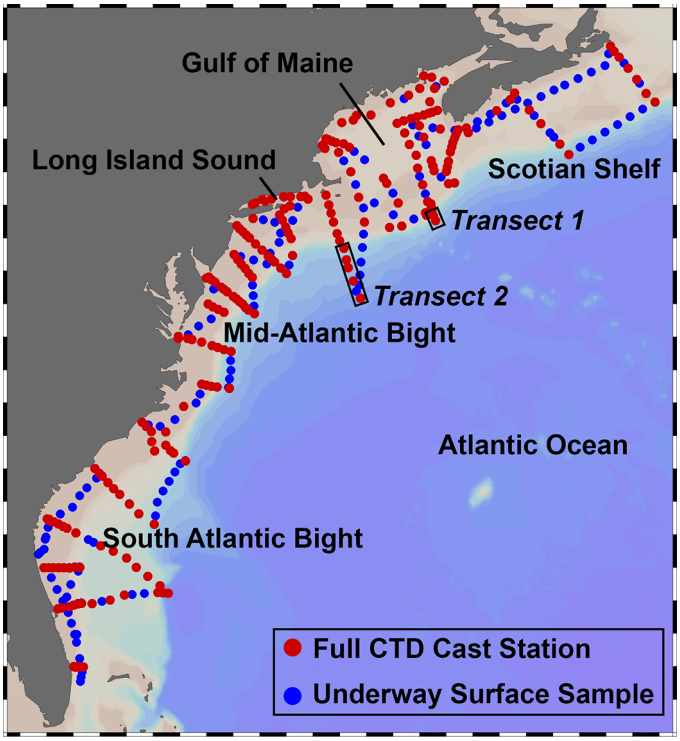

3.tif

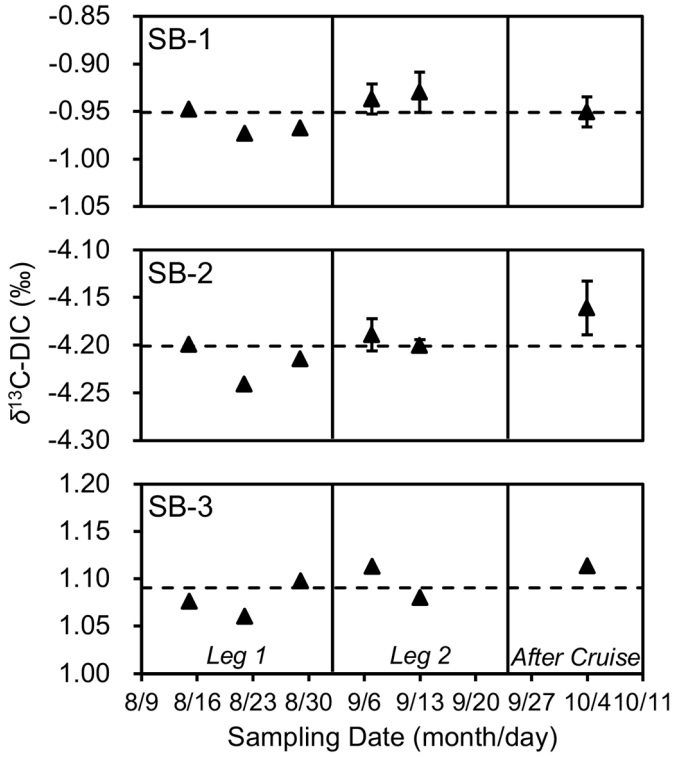

4.tif

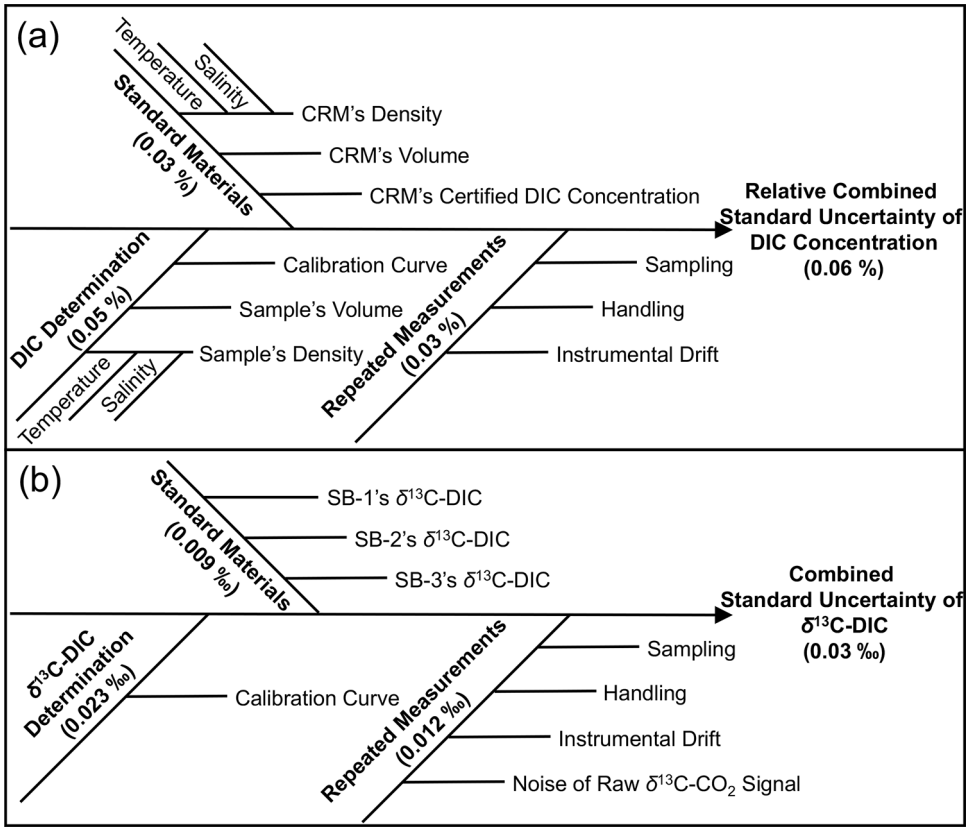

5.tif

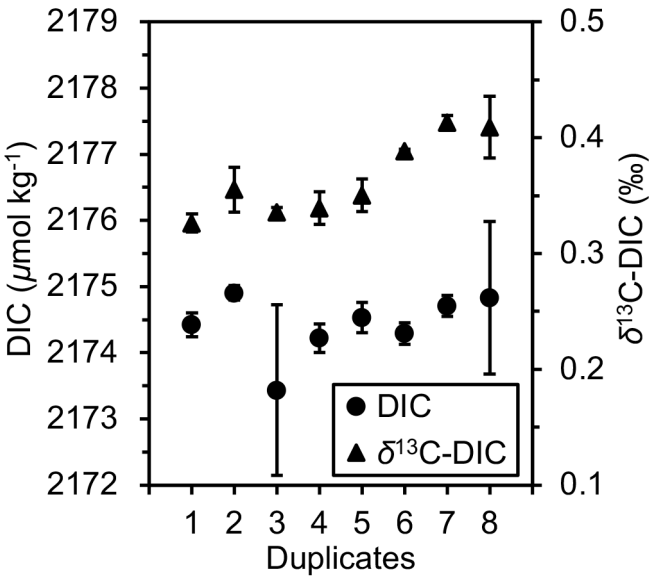

6.tif

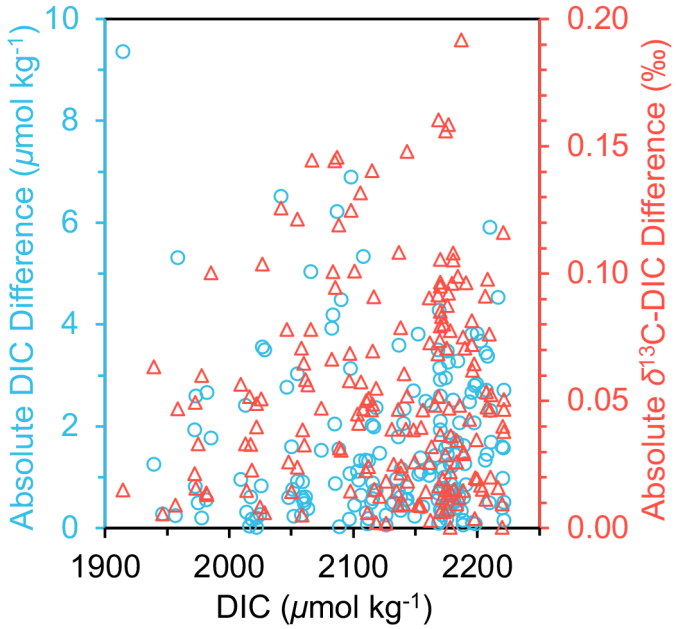

7.tif

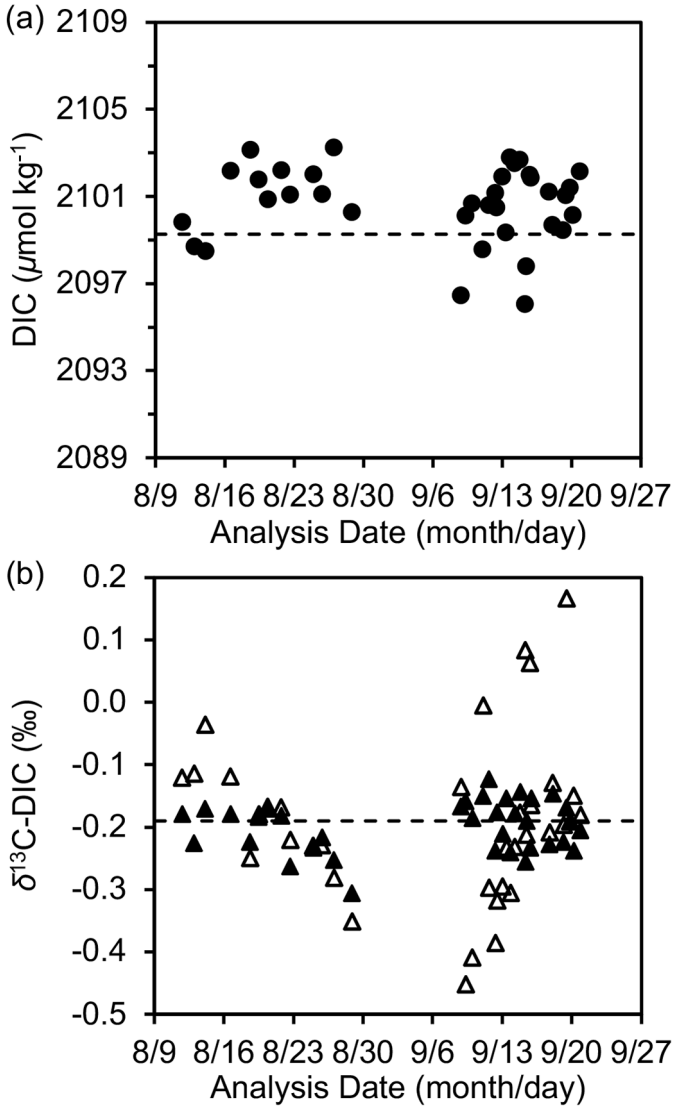

8.tif

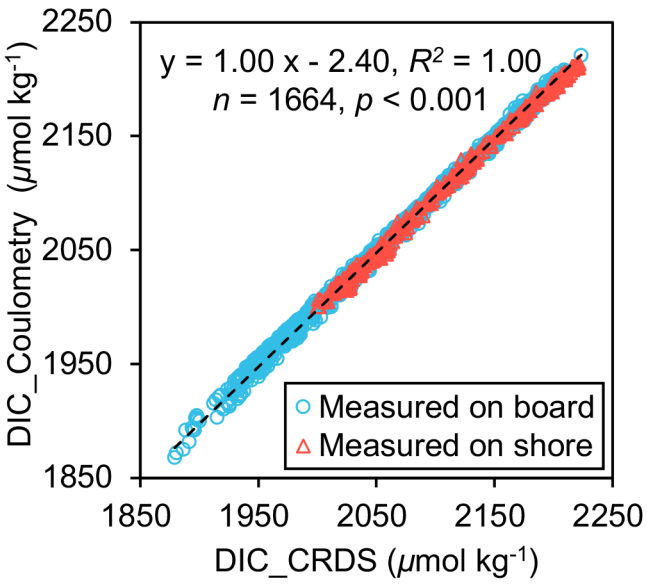

9.tif

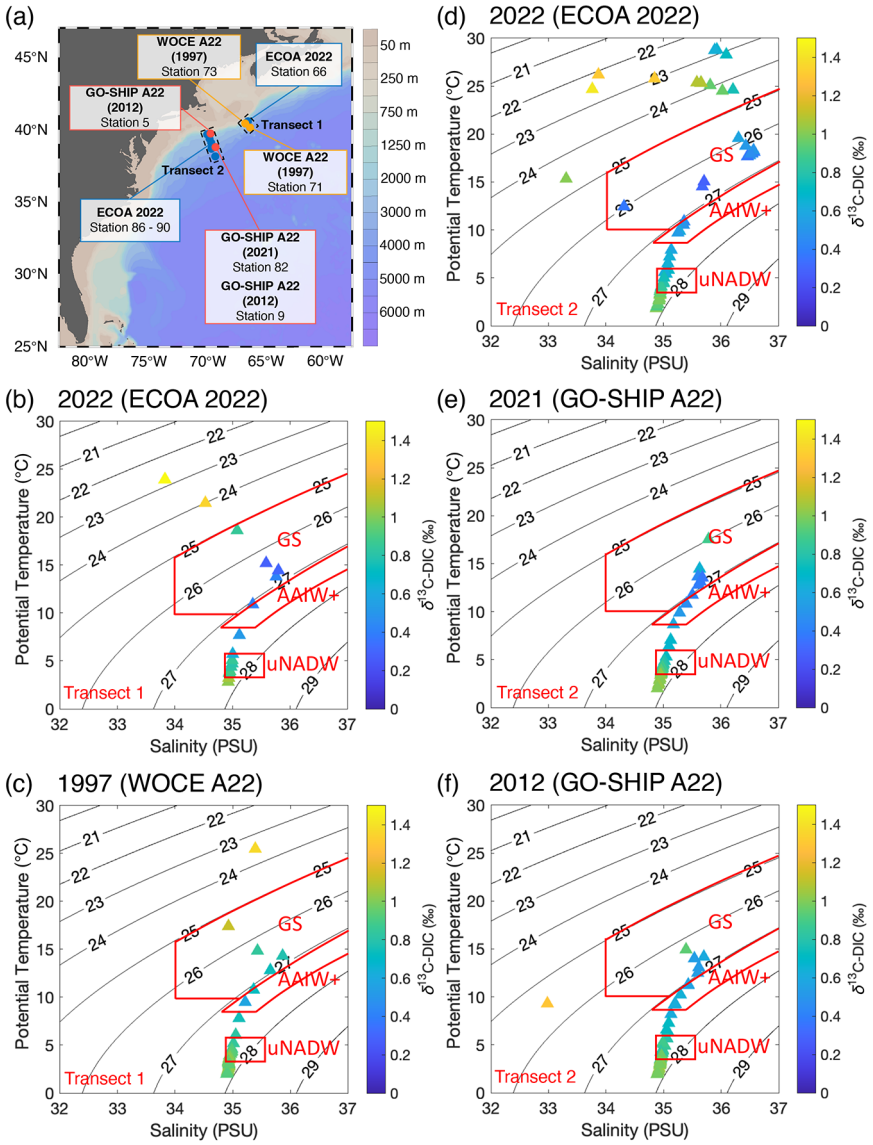

10.tif

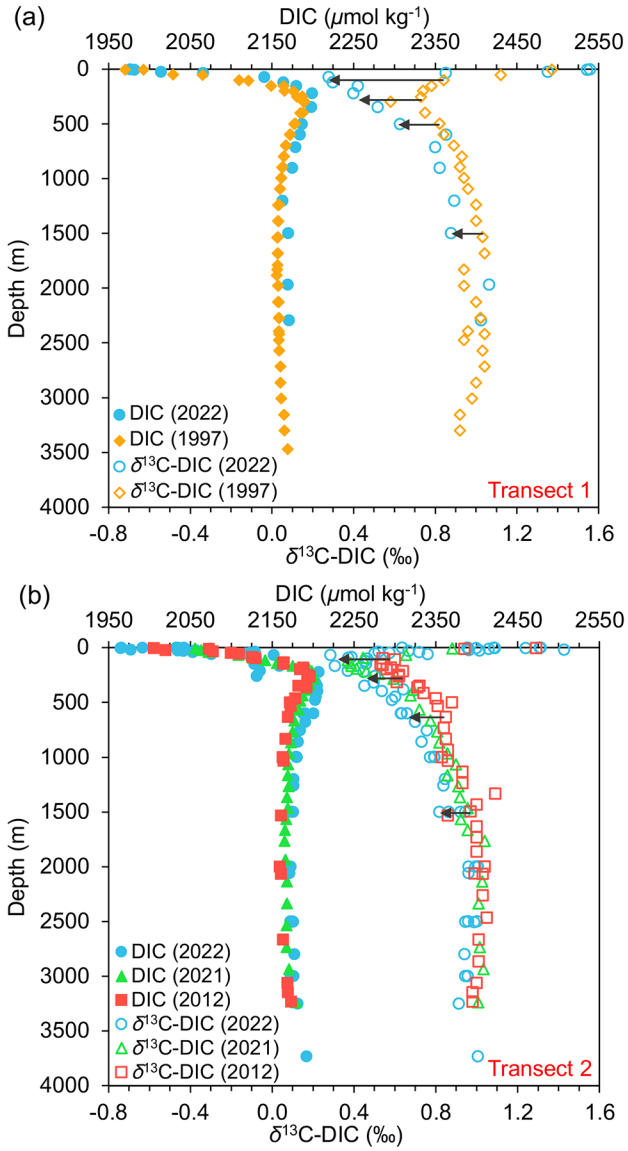

11.tif